Behavioral/Systems/Cognitive

Inducible Prostaglandin E_2 Synthesis Interacts in a Temporally Supplementary Sequence with Constitutive Prostaglandin-Synthesizing Enzymes in Creating the Hypothalamic–Pituitary–Adrenal Axis Response to Immune Challenge

Louise Elander,[1] Linda Engström,[1] Johan Ruud,[1] Ludmila Mackerlova,[1] Per-Johan Jakobsson,[2] David Engblom,[1] Camilla Nilsberth,[1] and Anders Blomqvist[1]

[1]Division of Cell Biology, Department of Clinical and Experimental Medicine, Faculty of Health Sciences, Linköping University, S-581 85 Linköping, Sweden, and [2]Division of Rheumatology, Department of Medicine, Karolinska Institute, 171 76 Stockholm, Sweden

Inflammation-induced activation of the hypothalamic–pituitary–adrenal (HPA) axis has been suggested to depend on prostaglandins, but the prostaglandin species and the prostaglandin-synthesizing enzymes that are responsible have not been fully identified. Here, we examined HPA axis activation in mice after genetic deletion or pharmacological inhibition of prostaglandin E_2-synthesizing enzymes, including cyclooxygenase-1 (Cox-1), Cox-2, and microsomal prostaglandin E synthase-1 (mPGES-1). After immune challenge by intraperitoneal injection of lipopolysaccharide, the rapid stress hormone responses were intact after Cox-2 inhibition and unaffected by mPGES-1 deletion, whereas unselective Cox inhibition blunted these responses, implying the involvement of Cox-1. However, mPGES-1-deficient mice showed attenuated transcriptional activation of corticotropin-releasing hormone (CRH) that was followed by attenuated plasma concentrations of adrenocorticotropic hormone and corticosterone. Cox-2 inhibition similarly blunted the delayed corticosterone response and further attenuated corticosterone release in mPGES-1 knock-out mice. The expression of the c-*fos* gene, an index of synaptic activation, was maintained in the paraventricular hypothalamic nucleus and its brainstem afferents both after unselective and Cox-2 selective inhibition as well as in Cox-1, Cox-2, and mPGES-1 knock-out mice. These findings point to a mechanism by which (1) neuronal afferent signaling via brainstem autonomic relay nuclei and downstream Cox-1-dependent prostaglandin release and (2) humoral, CRH transcription-dependent signaling through induced Cox-2 and mPGES-1 elicited PGE_2 synthesis, shown to occur in brain vascular cells, play distinct, but temporally supplementary roles for the stress hormone response to inflammation.

Key words: **CRH; ACTH; corticosterone; mPGES-1; LPS; Fos**

Introduction

Immune-induced activation of the hypothalamic–pituitary–adrenal (HPA) axis with increased release of adrenocorticotropic hormone (ACTH) and corticosteroids is critical for the fine-tuning of the inflammatory response (Besedovsky et al., 1986). It has been suggested that this activation is regulated by prostaglandins because it is attenuated after administration of cyclooxygenase (Cox) inhibitors (Krymskaya et al., 1987; Katsuura et al., 1988; Morimoto et al., 1991; Dunn and Chuluyan, 1992; Watanobe et al., 1998), although conflicting data also exist (Turnbull and Rivier, 1999).

Several lines of evidence indicate that prostaglandin E_2 (PGE_2) is the prostanoid involved. These include findings that injection of PGE_2 into the brain elicits ACTH release (Katsuura et al., 1990; Watanabe et al., 1990; McCoy et al., 1994) and that mice with targeted deletions of PGE_2 receptor subtypes EP_1 and EP_3 display impaired ACTH response to bacterial endotoxin (Matsuoka et al., 2003). However, PGE_2 is produced both under constitutive conditions and in response to homeostatic challenges, and the role of different PGE_2-synthesizing pathways in the immune-elicited activation of the HPA axis as well as the signaling routes remain to be clarified. Constitutive PGE_2 production occurs preferentially via Cox-1, whereas the induced PGE_2 formation is mediated by Cox-2. In both cases, an intermediate, PGH_2, is synthesized, which is the substrate for the prostanoid-specific terminal enzymes. For PGE_2, several terminal enzymes have been identified, among them the inducible microsomal prostaglandin E

Received Oct. 30, 2008; revised Dec. 19, 2008; accepted Dec. 30, 2008.

This work was supported by grants from the Swedish Research Council–Medicine (7879, 20535, 20725), the Swedish Cancer Foundation (4095), the Swedish Brain Foundation, Konung Gustaf V:s 80-årsfond, and the County Council of Östergötland. We thank Dr. Martin Hallbeck for technical advice.

Correspondence should be addressed to Dr. Anders Blomqvist, Division of Cell Biology, Department of Clinical and Experimental Medicine, Faculty of Health Sciences, Linköping University, S-581 85 Linköping, Sweden. E-mail: anders.blomqvist@liu.se.

DOI:10.1523/JNEUROSCI.5247-08.2009

 0270-6474/09/291404-10$15.00/0

synthase-1 (mPGES-1), shown to be critical for the febrile response during inflammation (Engblom et al., 2003; Saha et al., 2005) and for cytokine-elicited anorexia (Pecchi et al., 2006; Elander et al., 2007).

In the present study, we addressed the role of different PGE_2-synthesizing pathways for the HPA axis activation in mice with deletion of the gene encoding Cox-1, Cox-2, and mPGES-1, respectively, as well as in mice treated with unselective or Cox-2 selective inhibitors. The mice were injected intraperitoneally with lipopolysaccharide (LPS), and plasma levels of ACTH and corticosterone were monitored. Furthermore, to elucidate which structures involved in the activation of the stress hormone response were sensitive to induced PGE_2 synthesis, corticotropin-releasing hormone (CRH) gene expression in the hypothalamus was examined, as was the expression of the immediate-early gene c-*fos* [an index of synaptic activation (Hunt et al., 1987; Luckman et al., 1994)] in the paraventricular hypothalamic nucleus (PVH) and upstream brainstem regions, including catecholamine-expressing medullary neurons (Ericsson et al., 1994). The results show that the sustained immune-induced ACTH and corticosterone release occurs in response to induced PGE_2 synthesis, known to take place in brain vascular cells (Ek et al., 2001) and that it is associated with blunted CRH gene transcription. In contrast, the rapid response is independent of induced PGE_2 synthesis by Cox-2 and mPGES-1, and probably elicited by Cox-1. The findings imply that constitutive and induced prostaglandin-synthesizing enzymes act in a temporally supplementary sequence, involving neural and humoral routes, respectively, in creating the HPA axis response to inflammation.

Materials and Methods

Animals and tissue collection. All experimental procedures were approved by the Animal Care and Use Committee at Linköping University. They were performed on adult mice of the following strains: *Ptgs1*$^{-/-}$ [Cox-1 knock-out (KO)] and *Ptgs2*$^{-/-}$ (Cox-2 knock-out) and their respective wild-type littermates on a mixed B6;129P2 background (Morham et al., 1995; Langenbach et al., 1997), obtained by our own heterozygous breeding (breeding pairs were a gift from Robert Langenbach, National Institute of Environmental Health Sciences, Research Triangle Park, NC); *Ptgs2*$^{-/-}$ mice on a mixed B6;129P2 background (Morham et al., 1995), with separately bred wild-type mice of the same background used as controls (from Taconic); *Ptges*$^{-/-}$ (mPGES-1 knock-out) mice on a DBA/lacJ background (Trebino et al., 2003), which were generated both by homozygous breeding, in which case wild-type controls on the same background were used, and by heterozygous breeding on a line that had been backcrossed for six generations with DBA/lacJ wild-type mice, with wild-type littermates serving as controls; and wild-type C57/B6 mice (Scanbur). The animals were housed one to a cage in a pathogen-free facility at 20°C with a regular 12 h light/dark cycle (lights on, 7:00 A.M.; lights off, 7:00 P.M.). Food and water were provided *ad libitum*. In the morning (between 8:00 and 11:00 A.M.), the animals were given an intraperitoneal injection of 2 μg of lipopolysaccharide (LPS) (Sigma-Aldrich; 0111:B4) diluted in 100 μl of saline, or as control, saline only. In some experiments, animals were given an intraperitoneal injection of either an unselective Cox inhibitor [indomethacin (Confortid; Alpharma); 10 mg/kg] or a Cox-2 selective inhibitor [parecoxib (Dynastat; Pfizer), 10 mg/kg], 20 min before the LPS injection, or injected with vehicle. Because of the kinetics of parecoxib, the injection was repeated after 3 h, when applicable. The animals were killed by asphyxiation with CO_2 at various time intervals. For plasma protein assays, blood was immediately withdrawn from the right ventricle by heart puncture, collected in EDTA-covered containers (Sarstedt) and centrifuged at 7000 × *g* (4°C; 7 min) to obtain plasma, which was stored in aliquots at −70°C. For gene expression analysis with real-time reverse transcription (RT)-PCR, the brain was quickly removed, fresh-frozen on dry ice, and stored at −70°C. For immunohistochemistry and *in situ* hybridization, the animals were perfused through the left ventricle with 100 ml of saline, followed by 200 ml of 4% paraformaldehyde in phosphate buffer (0.1 M; pH 7.4; 4°C). The brain was removed, postfixed for 3 h, immersed in 30% sucrose in PBS (0.1 M; pH 7.4) overnight at 4°C, and cut in the transverse plane at 20 μm on a freezing microtome. Sections were collected in four series in cold cryoprotectant (0.1 M PBS containing 30% ethylene glycol and 20% glycerol) and stored until use at −20°C.

Corticosterone, ACTH, interleukin-1β, interleukin-6, and tumor necrosis factor α protein assays. For detection of corticosterone, plasma was thawed on ice and analyzed using an enzyme immunoassay (IDS OCTEIA corticosterone kit), according to the manufacturer's instructions. Using a 4-PL curve fit, a standard curve with an R value of 1.000 was obtained. The corticosterone antibody was generated in rabbit with an antigen consisting of corticosterone conjugated to BSA via a CMO [(*O*-carboxymethyl)oxime] group introduced synthetically at C3 of the steroid A chain. Assay sensitivity was 0.55 ng/ml. The kit antiserum showed the following cross-reactivity: 6.60% 11-dehydrocorticosterone; 5.93% 11-deoxycorticosterone; 1.39% progesterone; 0.85% cortisol; 0.60% prednisolone; 0.34% 21-deoxycortisol; 0.21% 5α-pregnan-3,20-dione; and <0.07% cross-reactivity with the following analytes: tetrahydrocortisone, dexamethasone, dehydroepiandrosterone, prednisone, pregnantriol, 20β-hydroxypregesterone, 4-pregnen-20βα-ol-3-one, estriol, estradiol, estrone, pregnenolone, 17α-hydroxypregnolone, cortisone, testosterone, 11-desoxycortisol, aldosterone, 17α-hydroxyprogesterone, and tetrahydrocortisol. The concentrations of ACTH, interleukin-6 (IL-6), and tumor necrosis factor α (TNFα) in plasma were determined using a bead-based multiplex analysis kit (Millipore; catalog #MBN1A-41K-04; lot 16522), using the Luminex-100 system (Luminex), as described in detail previously (Ruud and Blomqvist, 2007). Plasma IL-1β was measured separately (Millipore; catalog #MCYTO-70K-01; lot 16523), using the same system. For ACTH, a synthetically synthesized hormone was used as immunogen, whereas for cytokines the full recombinant protein, expressed in *Escherichia coli*, was used. Two separate quality control samples, supplied by the manufacturer and including all analytes, yielded results within the expected concentration range. The minimum detection concentrations for IL-1β, IL-6, TNFα, and ACTH were 1.6, 0.6, 1.0, and 1.9 pg/ml, respectively.

Real-time RT-PCR. RNA was extracted using QIAGEN RNeasy Lipid Mini kit (QIAGEN) according to the manufacturer's instructions. The concentrations and purity of the RNA were measured with NanoDrop ND-1000 Spectrophotometer (NanoDrop Technologies). A sample of 340 ng of RNA from the hypothalamus, dissected as described by Reyes et al. (2003), was reversely transcribed using SuperScript III First-Strand Synthesis kit with random hexamer primers in a volume of 20 μl, according to the manufacturer's protocol (Invitrogen). The efficiency of the RT reaction was evaluated by running five different RT reactions containing different amounts of RNA, which rendered a linear standard curve in real-time PCR using glyceraldehyde-3-phosphate dehydrogenase (GAPDH) and β-actin assays (see below). Real-time RT-PCR analyses were made using instruments, disposables, and chemicals from Applied Biosystems and were performed as singleplex reactions on 10 ng of cDNA in a 96-well format on Fast 7500 Real-Time PCR System, using the TaqMan Fast Universal PCR Master Mix (total reaction volume, 15 μl). GAPDH and β-actin were chosen as endogenous controls, after we had verified that their expression did not differ between treatment groups or genotypes (data not shown). All gene expression data were verified against both control genes. The following TaqMan Gene Expression Assays were used: *Gapdh* (Mm99999915_g1), *Actb* (β-actin) (Mm00607939_s1), *Crh* (Mm01293920_s1), and *Fos* (Mm00487425_m1). Gene expression was calculated using the ΔΔCt method (Ct, threshold cycle), where ΔCt for each target gene was calculated as $\Delta Ct_{(target)} - \Delta Ct_{(endogenous\ control)}$ and ΔΔCt as $\Delta Ct_{(mean,\ stimulated)} - \Delta Ct_{(mean,\ controls)}$. The relative upregulation or downregulation of gene expression was then calculated as $2^{-(\Delta\Delta Ct)}$ with SEM obtained by first calculating the SD for the stimulated group (s_1) and the control group (s_2), and then applying these values in the following formula: $[(s_p^2(1/n_1 + 1/n_2)]^{0.5}$, in which $s_p^2 = [s_1^2(n_1 - 1) + s_2^2(n_2 - 1)/(n_1 + n_2 - 2)$.

Immunohistochemistry. Every third section throughout the brain was

stained for Fos-like immunoreactivity (rabbit anti-Fos 1/1000; Santa Cruz Biotechnology; lot 10503; affinity-purified polyclonal rabbit antiserum raised against a synthetic peptide consisting of amino acids 3–16 at the N-terminal part of Fos of human origin) using the avidin–biotin–horseradish peroxidase complex methodology, as described in detail previously (Ruud and Blomqvist, 2007). To permit comparison between mice given different treatment (LPS/saline) and being of different genotypes (wild-type/knock-out), sections from all groups were processed simultaneously. A dual-labeling immunohistochemical technique was used for detecting Fos expression in catecholaminergic neurons in the ventrolateral medulla oblongata. In brief, sections were incubated overnight (room temperature) in a mixture of rabbit anti-mouse monoclonal anti-tyrosine hydroxylase antibody (1/8000; ImmunoStar; lot 436017; raised against tyrosine hydroxylase purified from rat PC12 cells) and rabbit anti-Fos antibody. Bound primary antibody was detected by incubation with goat anti-mouse IgG antibody (1:120; Dako) and biotinylated goat anti-rabbit IgG antibody (1/1000; Vector Laboratories), followed first by monoclonal peroxidase anti-peroxidase complex (1:125; Dako) that was visualized with 0.02% 3,3′-diaminobenzidine tetrahydrochloride (Sigma-Aldrich) and 0.03% H_2O_2 to generate a brown cytoplasmic reaction product in tyrosine hydroxylase-expressing neurons, and then by avidin–biotin peroxidase complexes visualized with 3,3′-diaminobenzidine tetrahydrochloride and H_2O_2 as above, but with the addition of 2.25% nickel ammonium sulfate, yielding a black nuclear staining in Fos-expressing cells. Specificity of the anti-Fos antibody was assessed as described in detail previously (Ruud and Blomqvist, 2007). Specificity of the tyrosine hydroxylase antibody was assessed by comparison of labeling patterns with the consensus distribution of dopamine-β-hydroxylase immunoreactivity, and by the absence of cross-reactivity against other catecholamine- and indolamine-synthesizing enzymes, according to the manufacturer's Western blot analysis.

Analysis of the labeling was done by an observer that was blinded to genotype and treatment of the animal. Nuclear groups were defined under dark-field illumination, using fiber tracts and the contrast between cell groups generated by differences in cell size and packing density as well as fiber content in the neuropil for cytoarchitectonic delineations. Estimates of dual labeling for tyrosine hydroxylase and Fos protein were done on neurons in the ventrolateral medulla oblongata, in a rostrocaudal region limited by the pyramid decussation and the rostral pole of the nucleus ambiguous (i.e., the region that has been shown to project to the PVH) (Sawchenko and Swanson, 1982).

In situ *hybridization.* For detection of CRH transcription, a 519-bp-long intron fragment of the preproCRH gene (GenBank accession no. NC_000069) was cloned by using PCR with specific primers corresponding to nucleotides 284–304 (forward primer, 5′-ctgtgccttaaaattccgatg-3) and 802–782 (reverse primer, 5′-tgggggagaaaggtaagattg-3; Cybergene). Mouse genomic DNA (300 ng; Promega) was used as template. The fragment was amplified for 40 cycles (45 s at 95°C, 45 s at 57°C, and 60 s at 72°C) and subsequently cloned into a pDRIVE vector (QIAGEN). The identity of the cloned fragment was confirmed by sequencing of both strands. A riboprobe was transcribed using Sp6 polymerase (antisense) in the presence of [^{33}P]UTP (PerkinElmer Life and Analytical Sciences) after linearization with *Bam*HI (Promega).

A probe complementary to c-*fos* mRNA was generated from a c-*fos* cDNA PBSsk$^+$ vector with a 2.1 kb insert corresponding to the entire c-*fos* coding region (Curran and Morgan, 1985), which was linearized with *Sma*I and transcribed with T7 polymerase, also in the presence of [^{33}P]UTP.

Unincorporated nucleotides were removed by using Quick Spin columns (Roche) according to the manufacturer's instructions. The *in situ* hybridization and autoradiography were performed as previously described (Engström et al., 2003). Briefly, every fourth section through each brain was mounted on Superfrost Plus slides (Menzel-Gläser), vacuum dried overnight, and postfixed in 4% paraformaldehyde for 30 min. The sections were then incubated at 37°C in proteinase K (10 μg/ml) for 30 min, dehydrated in graded concentrations of ethanol, and vacuum dried for ~3 h at room temperature. The hybridization solution (0.5 mg/ml tRNA, 0.1 M dithiothreitol, 50% formamide, 10% dextran sulfate, 2% Denhardt's solution, 0.3 M NaCl, 10 mM Tris, and 1 mM ethylenediamine-tetra-acetic acid, pH 8.0) contained a final probe activity of 1×10^7 cpm/ml. A total of 150 μl of this solution was applied on each slide, which was then coverslipped and sealed with DPX (VWR International). The sections were hybridized at 60°C for 48 h, rinsed in 4× standard saline citrate (SSC) buffer, pH 7.0, and incubated at 37°C with RNase A (20 μg/ml) for 30 min, followed by 0.1× SSC at 74°C for 30 min. They were then dehydrated, defatted in xylene, and vacuum dried at room temperature for at least 30 min before being dipped into Kodak NTB-2 nuclear track emulsion (Kodak). After 10–14 d of exposure, the slides were developed in D-19 developer (Kodak), fixed, and coverslipped.

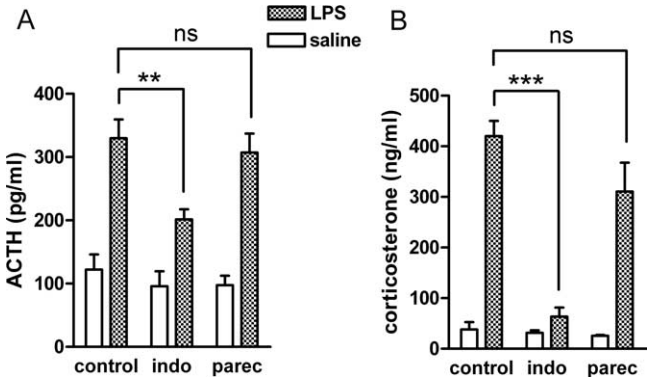

Figure 1. Effects of cyclooxygenase inhibition on ACTH (***A***) and corticosterone (***B***) release, 1 h after immune challenge. Wild-type mice were injected with indomethacin (indo) (10 mg/kg, i.p.) or parecoxib (parec) (10 mg/kg, i.p.) or, for controls, vehicle, 20 min before an intraperitoneal injection of 2 μg of LPS or saline. Because of its kinetics, the injection of parecoxib was repeated after 3 h. $n = 7–8$ for animals given LPS and $n = 5$ for those given saline. Error bars indicate SEM. $^{**}p < 0.01$ and $^{***}p < 0.001$ between treatments. ns, Not significant.

Quantification of the autoradiographic signal, as seen under dark-field illumination, was performed over the PVH by a blinded observer, using the ImageJ software (version 1.23; W. Rasband, National Institutes of Health, Bethesda, MD). In each animal, the optical density on both sides of PVH was calculated from digital micrographs (taken with a 10× objective, and with a fixed exposure time) of the section that displayed the strongest labeling, as determined qualitatively. Illumination was set so that pixel saturation was avoided and kept constant through the series of measurements. The obtained values were then subtracted from background values in adjacent regions devoid of specific signal.

Statistical analyses. All statistical analyses were performed in SPSS, version 12.01 (SPSS), or Microsoft Excel 2003 (Microsoft). For comparisons between several groups, data were analyzed with ANOVA, followed by *post hoc t* test, using the Bonferroni correction. For other data, Student's *t* test was used. A value of $p < 0.05$ was considered significant.

Results

Cyclooxygenase inhibition of LPS-induced ACTH and corticosterone release

The effect of unselective Cox inhibition and of Cox-2 selective inhibition on the early ACTH and corticosterone response is shown in Figure 1, *A* and *B*. Treatment of wild-type mice (of the C57/B6 strain) with a selective Cox-2 inhibitor, parecoxib, given intraperitoneally 20 min before LPS in a dose that extinguishes the febrile response in this experimental paradigm (data not shown), only marginally reduced the LPS-induced ACTH and corticosterone response at 1 h, and this effect was not statistically significant. In contrast, treatment with an unselective Cox inhibitor, indomethacin, significantly attenuated the LPS-elicited ACTH release and almost completely extinguished the corticosterone response.

At 6 h after injection, a different picture emerged. Thus, both indomethacin and parecoxib attenuated corticosterone release at this time point (Fig. 2*A*). Notably, the unselective Cox inhibitor indomethacin was not more effective in reducing the corticoste-

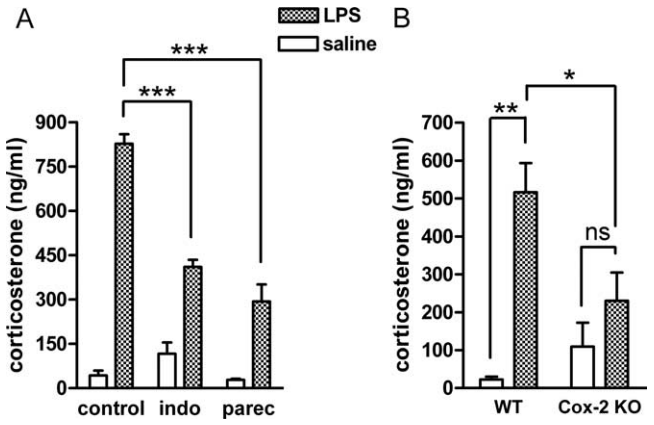

Figure 2. Effects of cyclooxygenase inhibition on corticosterone response 6 h after immune challenge. ***A***, Wild-type mice were injected with indomethacin (indo) (10 mg/kg, i.p.) or parecoxib (parec) (10 mg/kg, i.p.) or, for controls, vehicle, 20 min before an intraperitoneal injection of 2 μg of LPS or saline. Because of its kinetics, the injection of parecoxib was repeated after 3 h. $n = 7–8$ for animals given LPS and $n = 3$ for those given saline. ***B***, Wild-type and Cox-2 knock-out mice were injected intraperitoneally with 2 μg of LPS or saline. $n = 9–10$ for animals given LPS and $n = 3–4$ for those given saline. Error bars indicate SEM. $^*p < 0.05$, $^{**}p < 0.01$, and $^{***}p < 0.001$ between treatments and genotypes. ns, Not significant.

rone response than parecoxib, suggesting that Cox-1 does not contribute to this response. Notably, also, there was a tendency that indomethacin at this time point by itself elevated corticosterone levels. This is consistent with previous reports on a stimulatory effect of this drug on the HPA axis that occurs several hours after drug administration (Weidenfeld et al., 1983). The data from pharmacological inhibition of the Cox activity were further verified in Cox-$2^{-/-}$ mice (Fig. 2*B*). Although these mice tended to display higher basal plasma corticosterone concentration than wild-type mice, they were close to unresponsive to the LPS stimulus.

LPS-induced ACTH and corticosterone release in mPGES-$1^{-/-}$ mice

The ACTH and corticosterone responses were also examined in mPGES-1 knock-out mice, which previously have been shown to be devoid of induced PGE_2 synthesis on immune challenge (Engblom et al., 2003). Intraperitoneal injection of LPS (2 μg of LPS, i.p.) evoked a strong and similar increase of the ACTH concentration at 1 h after injection in knock-out and wild-type mice (Fig. 3*A*). However, at 3 h, the ACTH concentration had decreased in knock-out animals, whereas it remained high in the wild-type mice. At 6 h after injection, no difference was seen between the genotypes, both displaying low concentrations of ACTH.

Both genotypes showed equally strong corticosterone response to LPS at 1 and 3 h. However, at 6 h after injection, at which time point wild-type mice displayed the highest plasma concentration of corticosterone, the knock-out mice showed an attenuated response (Fig. 3*B*).

These data hence were consistent with those seen in mice subjected to Cox-2-selective inhibition. They suggest that, although inducible PGE_2 synthesis through Cox-2 and mPGES-1 is involved in the late corticosterone response to immune challenge, it plays little role for the rapid corticosterone release, which seems to be Cox-1 dependent.

To directly examine the contribution of Cox enzymes and mPGES-1, respectively, in the immune-induced corticosterone response at 6 h, we treated mPGES-1 knock-out mice with Cox inhibitors before challenging the mice with LPS. As shown in Figure 3*C*, parecoxib further reduced the corticosterone response, in addition to the attenuation that resulted from the gene deletion. In contrast, indomethacin treatment had no significant additive effect, a finding that may be explained by its corticosterone-releasing properties (Weidenfeld et al., 1983). Although the data suggest that mPGES-1 is coupled to Cox-2 in the late immune-induced corticosterone response, they also show that other terminal enzymes, in addition to mPGES-1, may play a role. From a technical perspective, note that the difference in corticosterone release observed at 6 h after injection between LPS-treated mPGES-1 knock-out and wild-type mice obtained from homozygous breeding (Fig. 3*B*) was corroborated in littermates obtained from animals that had been backcrossed to the parental strain (Fig. 3*C*, left bars)

Plasma levels of IL-1β, IL-6, and TNFα

Having established that induced PGE_2 production is involved in the late stress hormone response, we next examined several upstream components involved in this response to identify the underlying mechanisms. First, we measured plasma levels of the proinflammatory cytokines IL-1β, IL-6, and TNFα in LPS-challenged wild-type and mPGES-1 knock-out mice. These cytokines have previously been shown to play a role in the activation of the HPA axis (Turnbull and Rivier, 1999) and to affect central prostaglandin synthesis in inflammatory conditions (Cao et al., 1998; Ek et al., 2001). The findings are illustrated in Figure 4. As seen, plasma levels of IL-1β, IL-6, and TNFα were low or below detection limit in naive animals and there were no significant differences between genotypes. Also, the LPS-induced expression of IL-1β and IL-6 was similar between wild-type and knock-out mice. For TNFα, a small difference was seen between genotypes at 6 h after LPS injection ($p < 0.01$), a time point at which the TNFα level in both wild-type and mutant mice, however, was low. These data suggest that the effect of induced PGE_2 synthesis on ACTH and corticosterone release is likely to be exerted via a direct, central action. This is consistent with previous findings that intracerebral injection of PGE_2 produces increases in plasma ACTH concentration (Katsuura et al., 1990; Watanabe et al., 1990; McCoy et al., 1994), and with the demonstration of stimulatory G-protein-coupled PGE_2 receptors (such as EP_4) in the PVH, as well in structures known to influence hypophysiotropic neurons, such as the preoptic region and catecholaminergic cells in the ventrolateral medulla (Herman et al., 1996; Zhang and Rivest, 1999; Ek et al., 2000; Oka et al., 2000; Matsuoka et al., 2003).

CRH gene regulation

We next examined whether wild-type and mPGES-$1^{-/-}$ mice differed in the immune-induced expression of CRH mRNA. Quantitative real-time RT-PCR for CRH mRNA in the hypothalamus demonstrated significantly higher levels in LPS-injected wild-type mice compared with wild-type mice given saline, at 1 h after injection ($p < 0.05$), whereas no significant upregulation was seen in knock-out mice at this time point (Fig. 5*A*). There were also significantly higher CRH mRNA levels in the LPS-treated wild-type group than in the LPS-treated knock-out group ($p < 0.05$), whereas the CRH mRNA levels in saline-injected mice did not differ between genotypes. At 3 h, both genotypes displayed elevated levels of CRH mRNA after LPS injection compared with saline-injected controls; however, the data on wild-type mice were more consistent as is reflected by a smaller SE and higher statistical significance in that group.

We then used *in situ* hybridization of CRH heteronuclear (hn)

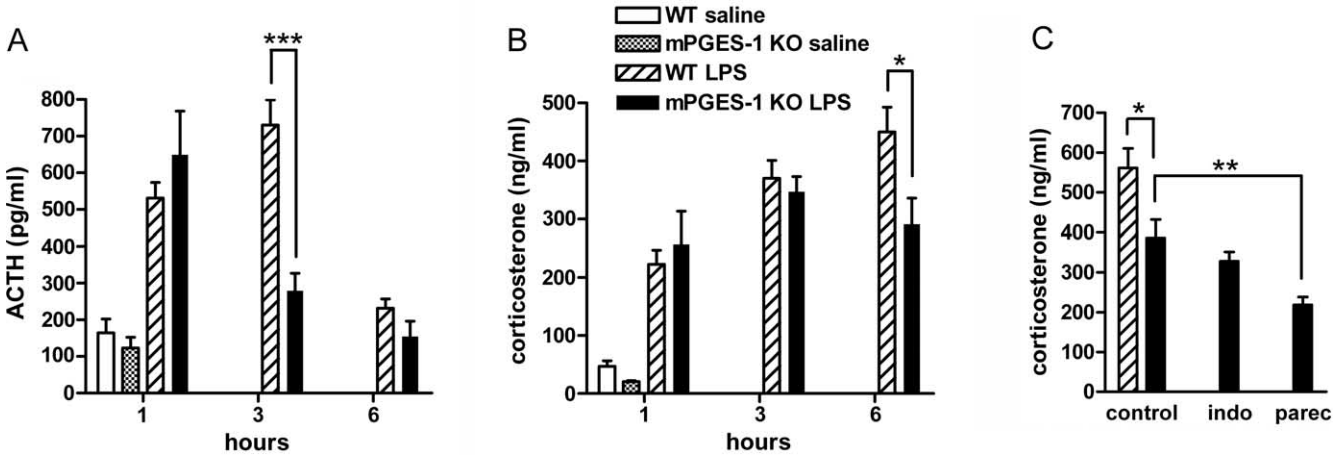

Figure 3. ACTH and corticosterone responses to immune challenge in mPGES-1 knock-out mice. Plasma concentrations of ACTH (***A***) and corticosterone (***B***) were examined after intraperitoneal injection of 2 μg of LPS (1, 3, and 6 h) or saline (1 h). $n = 6–12$ for each data point. ***C***, mPGES-1 knock-out mice were injected with indomethacin (10 mg/kg i.p.) or parecoxib (10 mg/kg i.p.) 20 min before an intraperitoneal injection of 2 μg of LPS. The parecoxib injection was repeated after 3 h, and serum corticosterone levels were determined at 6 h after LPS injection. Control wild-type and mPGES-1 knock-outs were given vehicle before injection with LPS. $n = 6–9$ for each treatment/genotype. Error bars indicate SEM. $^*p < 0.05$, $^{**}p < 0.01$, and $^{***}p < 0.001$ between treatments and genotypes.

RNA to examine whether the differences in CRH mRNA expression reflected differences in transcriptional regulation and, if so, where the transcriptional regulation took place. Wild-type and mPGES-1 $^{-/-}$ mice were injected with saline or LPS, and transcriptional activity in the hypothalamus was examined after 1 h by autoradiographic detection of a ^{33}P-labeled riboprobe complementary to a 519-bp-long intronic sequence of the CRH gene. After saline injection, both genotypes displayed only weak CRH hnRNA signal in the PVH (Fig. 5*B*,*D*). As reported previously (Rivest et al., 1995), immune challenge with LPS resulted in wild-type mice in upregulation of the CRH hnRNA signal in this nucleus; however, little upregulation was seen in LPS-treated mPGES-1 knock-out mice (Fig. 5*C*,*E*). This difference was verified by quantitative densitometric measurements, which demonstrated a 4.5-fold increased CRH hnRNA expression in the PVH of immune-challenged wild-type mice compared with saline-treated wild-type mice ($p < 0.01$; $n = 5$ and 3, respectively), whereas no significant difference between treatment groups was seen among mPGES-1 KO mice ($p = 0.26$; $n = 6$ and 3, respectively). No induced CRH hnRNA expression was seen in other parts of the hypothalamus, being consistent with previous observations (Rivest et al., 1995).

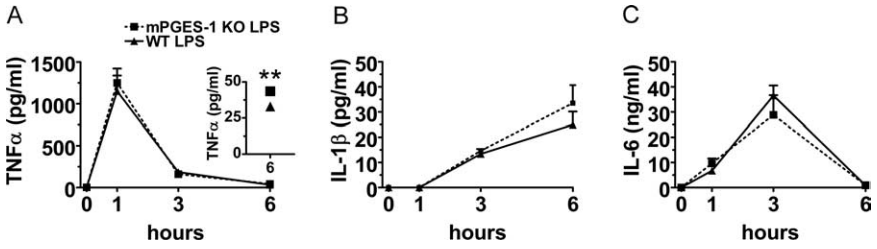

Figure 4. Plasma concentrations of TNFα (***A***), IL-1β (***B***), and IL-6 (***C***) in wild-type (WT) and mPGES-1 KO mice before, and 1, 3, and 6 h after intraperitoneal injection of 2 μg of LPS. Except for a small difference in the TNFα levels at 6 h (***A***, inset), there were no statistically significant differences between genotypes. $n = 3–5$ for the 0 h data points, and 8–11 for the 1, 3, and 6 h data points. Error bars indicate SEM. $^{**}p < 0.01$ between genotypes.

Expression of c-*fos* mRNA and protein in autonomic relay nuclei

As a final step, we examined neuronal activation, as seen by *in situ* hybridization for c-*fos* mRNA and immunohistochemical detection of Fos protein, in the paraventricular hypothalamus (Fig. 6) and several brainstem and forebrain autonomic relay nuclei in response to immune challenge with LPS (Figs. 7, 8). The Fos protein expression in the PVH in Cox-1 knock-out and wild-type mice are shown in Figure 6*A–C*, those in Cox-2 knock-out and wild-type mice are illustrated in Figure 6*D–F*, and those from mPGES-1 knock-out and wild-type mice are shown in Figure 6*G–I*. As seen, there was strong induction of Fos protein in LPS-treated animals 3 h after injection, regardless of genotype (Fig. 6*B*,*C*,*E*,*F*,*H*,*I*). Qualitative examination by a blinded observer suggested a stronger Fos labeling in knock-out mice than in wild-type mice, although this could not be verified statistically by cell counts, because of small sample size ($n = 3–4$) and considerable interindividual variation. *In situ* hybridization, performed on sections from mPGES-1 knock-out and wild-type mice killed 1 h after injection, showed strong induction of hybridization signal for c-*fos* mRNA by LPS in both genotypes (Fig. 6*K*,*L*), but again with a tendency to more pronounced labeling in the knock-out mice, as determined by qualitative examination. These observations were corroborated by quantitative real-time RT-PCR analysis of c-*fos* mRNA expression in the hypothalamus of wild-type and mPGES-1 knock-out mice ($n = 7–10$) at 1 h after intraperitoneal LPS injection. Whereas wild-type mice showed 2.6 times upregulation of c-*fos* mRNA after intravenous LPS compared with saline ($p < 0.001$), knock-out mice displayed 4.5 times upregulation of the c-*fos* transcript ($p < 0.001$), from a level that was similar to that of saline-treated wild-type mice. This difference in c-*fos* mRNA upregulation between genotypes was statistically significant ($p < 0.01$).

To further verify the findings of maintained Fos expression in the knock-out mice, we pretreated wild-type mice with indomethacin or parecoxib, before challenging them with LPS, and measured with real-time RT-PCR the c-*fos* mRNA level in the hypothalamus at 1 h. We found that neither unselective Cox-inhibition with indomethacin, nor selective Cox-2 inhibition

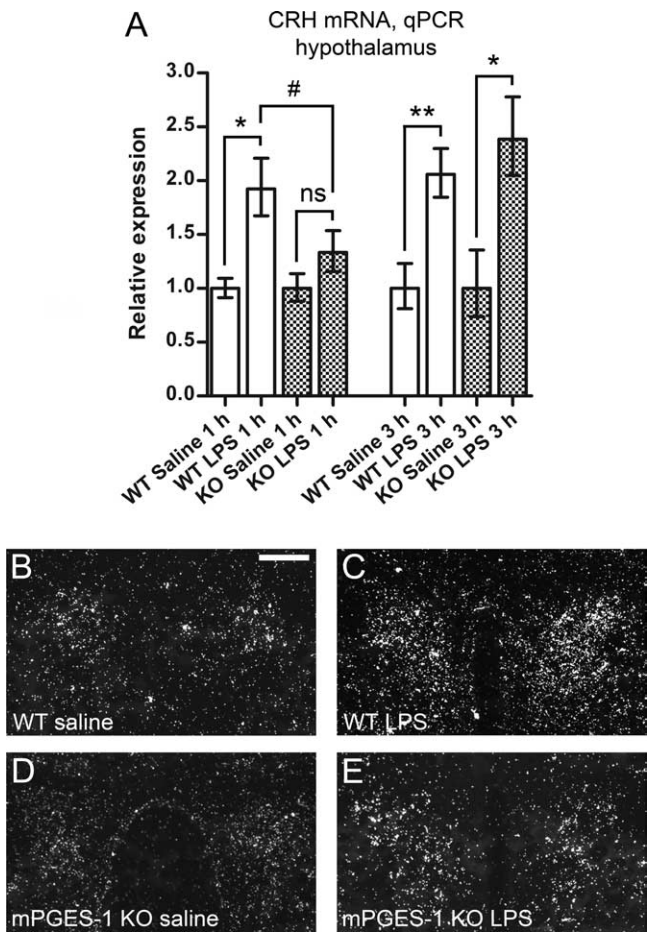

Figure 5. Attenuated CRH transcription and expression in mPGES-1 knock-out mice after immune challenge. ***A***, Quantitative RT-PCR of CRH mRNA expression in the hypothalamus after intraperitoneal injection with saline or 2 μg of LPS. Error bars indicate SEM. $n = 6–10$ for each group. $^*p < 0.05$ and $^{**}p < 0.01$ between LPS and saline injected mice; $^{\#}p < 0.05$ between LPS-injected WT and KO mice. ns, Not significant. ***B–E***, Dark-field micrographs showing *in situ* hybridization for CRH heteronuclear RNA in the paraventricular nucleus of the hypothalamus of wild-type (WT) and mPGES-1 KO mice 1 h after intraperitoneal injection with saline or 2 μg of LPS. Scale bar, 100 μm.

with parecoxib, inhibited the c-*fos* mRNA expression (Fig. 6*M*). Notably, and in contrast to what was found in mPGES-1 knock-out mice, the Cox-inhibited mice did not display significantly higher c-*fos* mRNA levels than saline-pretreated mice.

Examination of Fos expression in other regions known to be activated in response to immune stimuli, such as the nucleus of the solitary tract and the area postrema, the ventrolateral medulla (VLM), the parabrachial nucleus, the ventromedial preoptic nucleus, and the central nucleus of the amygdala (Elmquist et al., 1993, 1996; Wan et al., 1993), also showed LPS-induced induction in both wild-type and gene-deleted mice, with a tendency, as determined qualitatively, that the labeling was stronger in knock-out mice than in wild-type mice. Although illustrated for mPGES-1 wild-type and knock-out mice (Fig. 7), these micrographs are representative also for the findings in the Cox-1 and Cox-2 strains.

Because it is well established that catecholaminergic neurons in VLM are important for the immune-induced activation of the PVH (Weidenfeld et al., 1989; Ericsson et al., 1994; Buller et al., 2001; Schiltz and Sawchenko, 2007), and because PGE_2 has been suggested to activate these neurons (Ericsson et al., 1997), we specifically examined Fos protein expression in tyrosine hydroxylase-positive neurons in the VLM of wild-type and mPGES-1 knock-out mice, by using a dual-labeling immunohistochemical procedure. The results, shown in Figure 8, demonstrated that the percentage of tyrosine hydroxylase-positive neurons that also were positive for LPS-induced Fos expression was similar between genotypes.

Discussion

This study demonstrates that constitutive and induced prostaglandin synthesis play distinct roles for early and late phases, respectively, of the immune-elicited stress hormone response. Deletion/inhibition of Cox-2 attenuated the corticosterone release seen at 6 h after intraperitoneal administration of LPS, whereas no effect was observed on this response at 1 h. In contrast, pretreatment of mice with the unselective Cox inhibitor indomethacin that targets Cox-1 in addition to Cox-2 almost completely extinguished the early corticosterone response but was no more effective than selective Cox-2 inhibition in reducing the late corticosterone release. Furthermore, Cox-2 inhibition did not affect ACTH release at 1 h, whereas indomethacin strongly attenuated this early response. We conclude that induced prostaglandin synthesis, via Cox-2, contributes to the delayed HPA axis activation in this experimental paradigm, whereas constitutive prostaglandin synthesis, via Cox-1, is involved in the early response. Although this conclusion is based on deducing the role of Cox-1 from the differential responses to a nonselective Cox-inhibitor and a Cox-2 selective inhibitor, and ideally should be verified in Cox-1-inhibited mice, it is in strong accord with a similar complementary role for Cox-1 and Cox-2 in shaping the febrile response to LPS as well as the associated brain activation pattern (Zhang et al., 2003).

Although our data from mPGES-1 knock-out mice demonstrate that mPGES-1-derived PGE_2 is involved in the delayed HPA axis response, they also indicated that other prostaglandins may play a role. Hence, when mPGES-1 knock-out mice were treated with a Cox-2 selective inhibitor, LPS-induced corticosterone release was further attenuated. Indeed, it has been demonstrated that, in addition to PGE_2, PGE_1 and $PGF_{2\alpha}$ elicit ACTH release when injected systemically or into the brain (Katsuura et al., 1990; Nasushita et al., 1997); however, although *in vitro* studies have shown the release of these prostaglandin species from neural cells (Althaus and Siepl, 1997), their presence in the brain remains to be demonstrated.

Our data show that the effect of immune-induced PGE_2 synthesis on stress hormone release is associated with transcriptional activation of the CRH gene. Whereas immune challenge with LPS in wild-type mice resulted in increased expression of CRH hnRNA in the PVH and elevated levels of CRH mRNA, no corresponding changes were seen in mPGES-1 knock-out mice. Considering that peptide synthesis and release are estimated to occur ~60–90 min after stimulus-activated CRH gene transcription (Watts, 2005), the differences in CRH mRNA levels between genotypes 1 h after LPS injection will not influence ACTH release at that time point (and which was similar between genotypes), but fit temporally with the differences in plasma ACTH levels seen at 3 h, and with the effect of the gene deletion on corticosterone levels at a later time point. However, additional direct local effects of PGE_2 on CRH or corticosterone release (McCoy et al., 1994; Engström et al., 2008) may also play a role.

A second major finding of the present study is that the Cox-dependent activation of the HPA axis seems to be unrelated to or to occur downstream of the LPS-induced neural activation. Thus, Cox-1, Cox-2, or mPGES-1 knock-out mice, or mice treated with

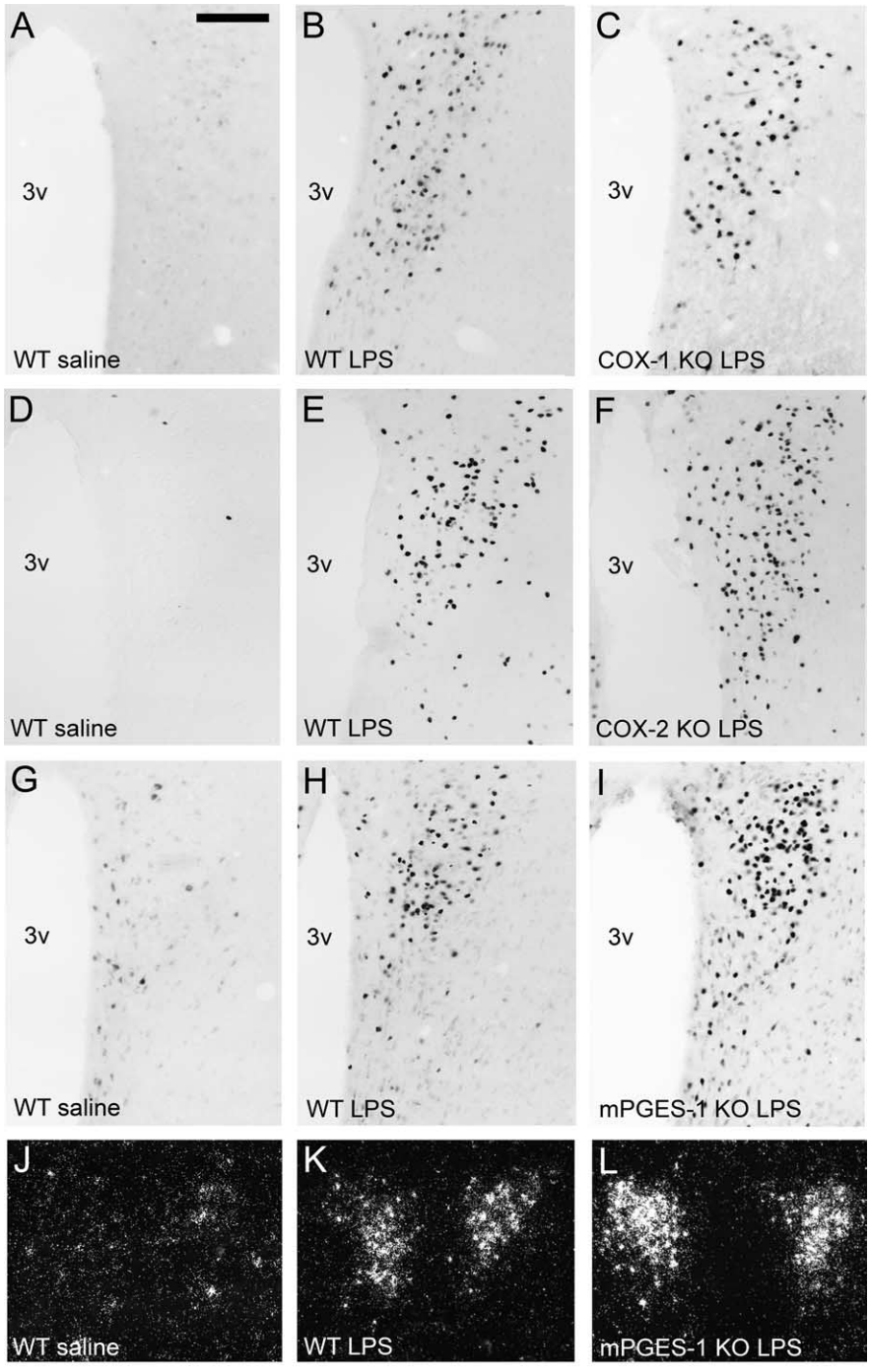

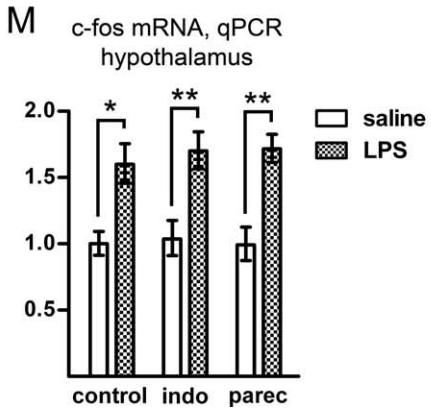

Cox inhibitors, did not show any attenuation of the c-*fos* expression in the PVH and hypothalamus, while displaying extinguished or attenuated stress hormone release. Our data hence indicate that the c-*fos* expression that occurs in these structures after intraperitoneal injection of LPS results from synaptic input through the vagus nerve via Cox- and mPGES-1-independent mechanisms. A role of vagus nerve signaling in the expression of c-*fos* after intraperitoneal injection is consistent with the finding that vagotomy or reversible inactivation of the vagus nerve blocked induction of c-*fos* by LPS given intraperitoneally, whereas it had no effect when the endotoxin was administered intravenously (Wan et al., 1994; Marvel et al., 2004).

Our observation that c-*fos* expression in PVH occurs also in the absence of Cox-2 and mPGES-1 is in good accord with the recent observations by Ching et al. (2007) in mice with targeted deletion of the IL-1 receptor type 1 in endothelial cells. These authors showed that c-*fos* expression in PVH in response to intraperitoneal, but not intravenous, administration of IL-1, was independent on endothelial cell IL-1R1 receptors, whereas induced Cox-2 expression in the brain was extinguished in mutant mice regardless of the route of cytokine administration, indicating the presence of a neuronal pathway for c-*fos* activation, which is not mediated by central Cox-2-dependent prostaglandin synthesis. Our finding that unselective Cox-inhibition with indomethacin, but not selective Cox-2 inhibition, attenuated/extinguished the early stress hormone response, while not inhibiting c-*fos* expression, adds to the observations by Ching et

←

Figure 6. Immune-induced expression of the c-*fos* gene in the hypothalamus of mice with deletion/inhibition of prostaglandin-synthesizing enzymes. ***A–I***, Immunohistochemical staining for Fos protein in the paraventricular hypothalamic nucleus in wild-type (WT) mice given saline (***A***, ***D***, ***G***), WT mice given an intraperitoneal injection of 2 μg of LPS (***B***, ***E***, ***H***), and Cox-1, Cox-2, and mPGES- KO mice given LPS (***C***, ***F***, ***I***), 3 h after injection. ***J–L***, c-*fos* mRNA expression in the paraventricular hypothalamic nucleus 1 h after injection in saline-treated WT mice (***J***), LPS (2 μg, i.p.)-treated WT mice (***K***), and LPS-treated mPGES-1 KO mice (***L***). 3v, Third ventricle. Scale bar: (in ***A***) ***A–I***, 100 μm; ***J–L***, 160 μm. ***M***, Real-time RT-PCR (qPCR) for c-*fos* mRNA in the hypothalamus. Bars show differences in c-*fos* mRNA concentrations between animals injected with LPS (2 μg, i.p.) or saline, and pretreated with vehicle (controls), indomethacin (indo), or parecoxib (parec). $n = 4$ in the saline-treated groups, and $n = 8$ in the LPS-treated groups. Error bars indicate SEM. $^*p < 0.05$ and $^{**}p < 0.01$ between LPS- and saline-injected mice of the same genotype.

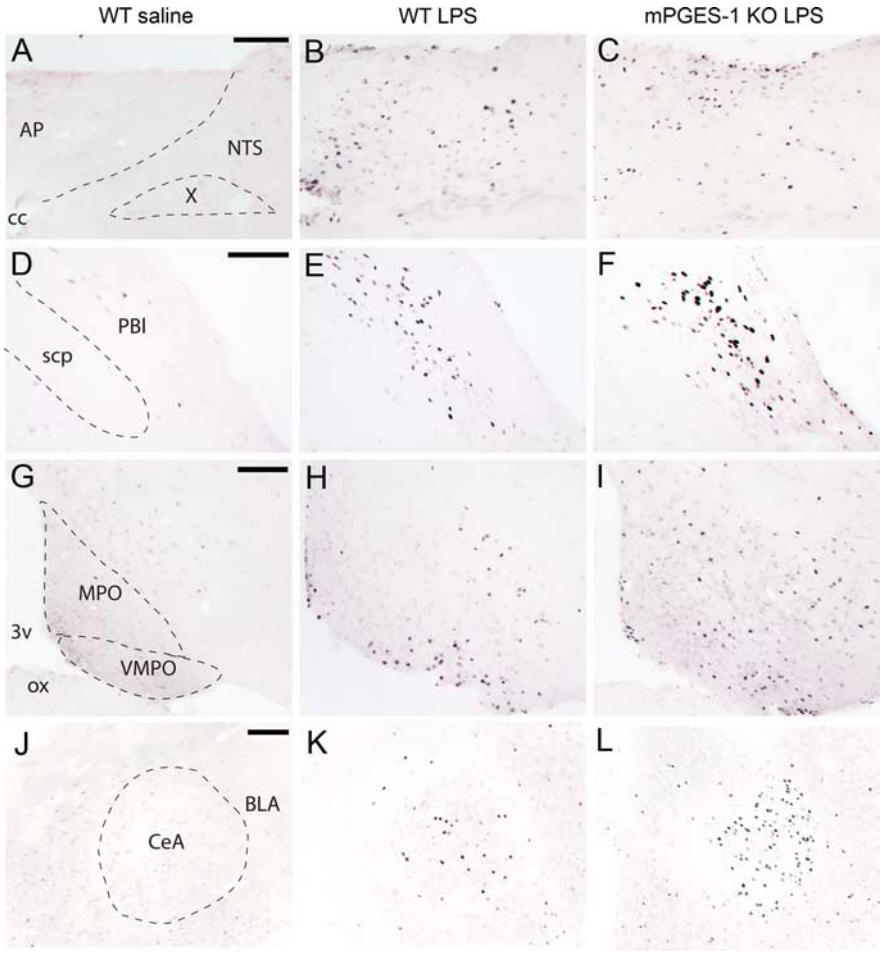

Figure 7. Immune-induced Fos-protein expression in brainstem and forebrain autonomic relay nuclei in mPGES-1 KO mice, 3 h after intraperitoneal injection of 2 μg of LPS. ***A–C***, Lower part of the brainstem showing the area postrema (AP) and solitary tract nuclear complex (NTS) in saline-injected controls (***A***), wild-type (WT) mice injected with LPS (2 μg, i.p.) (***B***), and KO mice injected with LPS (***C***). Midline is to the left and dorsal is upward. cc, Central canal; X, dorsal motor nucleus of the vagus nerve. ***D–F***, Part of the dorsolateral pons showing the lateral parabrachial nucleus (PBl) and superior cerebellar peduncle (scp). ***G–I***, Part of the preoptic region of the hypothalamus showing the ventromedial (VMPO) and median (MPO) preoptic nucleus. 3v, Third ventricle; ox, optic decussation. ***J–L***, Part of the temporal lobe showing the central (CeA) and basolateral (BLA) nucleus of the amygdala. Scale bars, 100 μm (in all panels).

al. (2007) by suggesting that that this neuronal pathway neither is Cox-1 dependent. It should be pointed out, however, that the independence of prostaglandin-synthesizing enzymes for the c-*fos* expression applies to the present experimental paradigm, and that other mechanisms, involving Cox enzymes, may be at play when the immune stimulus is delivered intravenously (Zhang et al., 2003; Ching et al., 2007), or when LPS is given intraperitoneally at doses that involve spread into the bloodstream (cf. Wan et al., 1994; Sagar et al., 1995; Lacroix and Rivest, 1997).

There is evidence that cytokines can activate the vagus nerve in both a prostaglandin-dependent and -independent manner; however, the PGE_2 receptors on the vagus nerve are of the EP_3 subtype (Ek et al., 1998), implying that they play an inhibitory role (Irie et al., 1993). The dissociation between c-*fos* expression and HPA axis activation that was seen in the present study after Cox-1 inhibition seems to indicate that Cox-1 is downstream of vagus nerve afferent signaling but upstream of CRH and/or ACTH release. Although the precise site of action of Cox-1 in the HPA axis response remains to be elucidated, it has been reported that cytokines instilled into the hypothalamic median eminence elicit an indomethacin-sensitive ACTH release (McCoy et al., 1994), implying a direct action of prostaglandins, and hence of prostaglandin-synthesizing enzymes at this site.

Our findings of maintained c-*fos* expression in mPGES-1 knock-out mice are clearly inconsistent with recent work by Dallaporta et al. (2007), who reported that Fos protein expression was extinguished in autonomic relay nuclei, including the PVH, in mPGES-1 knock-out mice challenged with LPS. We have no obvious explanation for this discrepancy, with the possible exception that the given dose of LPS (400 μg/kg) was approximately fourfold higher and of a different serotype than in the present study, whereas the time point after injection (3 h), as well as the route of administration (intraperitoneal), and the strain and origin of the mice (DBA1/lacJ) (Trebino et al., 2003) were similar. We can only note that our data on intact Fos protein expression in mPGES-1 knock-out mice were corroborated by *in situ* hybridization for c-*fos* mRNA in the PVH and of real-time RT-PCR analysis of c-*fos* mRNA expression in the hypothalamus, as well as by similar findings in Cox-1 and Cox-2 knock-out mice.

On an additional note, our data rather indicate that induced, centrally acting PGE_2 in fact attenuates the immune-induced Fos expression. We found that c-*fos* mRNA expression in the hypothalamus, as demonstrated by real-time RT-PCR, was not only maintained, but augmented, in the mPGES-1 knock-out mice, corroborating our qualitative observation that Fos protein expression tended to be stronger in the PVH and other autonomic relay nuclei in mPGES-1 knock-out mice than in wild-type mice. Although these tentative observations will require additional quantitative studies, an attenuated Fos expression by a direct central action of PGE_2, although contradictory to the fact that PGE_2 injected centrally induces Fos (Lacroix et al., 1996), would be consistent with the predominant EP_3 receptor expression in many brainstem autonomic relay nuclei (Ek et al., 2000; Engblom et al., 2001), because the most abundant isoform of the EP_3 receptor is coupled to inhibitory G-proteins that reduce cAMP levels (Irie et al., 1993; Vasilache et al., 2007). Therefore, as suggested by Zhang et al. (2003), if anything, PGE_2 binding to the EP_3 receptor may be expected to result in inhibition of these neurons [as is hypothesized for thermosensory preoptic neurons (Lazarus et al., 2007)] and hence reduced Fos expression, as indicated by the present results. The findings of attenuated Fos expression are also consistent with the negative feedback of PGE_2 on cytokine production in macrophage-like cells (Knudsen et al., 1986; Kunkel et al., 1988), which includes perivascular macrophages, and although the present data, except for a small late increase in TNFα, showed no difference in circulating cytokines between mPGES-1 knock-out and wild-type mice, we observed increased transcriptional regulation of IL-6 in the brain of mPGES-1 knock-out mice (Nilsberth et al., 2008). Although speculative, a negative-feedback mechanism involving

PGE_2, regardless of whether it is mediated directly by EP receptor binding or via attenuated central cytokine production, may help modulating the direct neuronally driven input onto the HPA axis, and would fit with the temporally supplementary roles by which neuronal afferent signaling via the vagus nerve and humoral signaling through induced central prostaglandin synthesis interact in creating the stress hormone response to inflammation, as shown by present experiments.

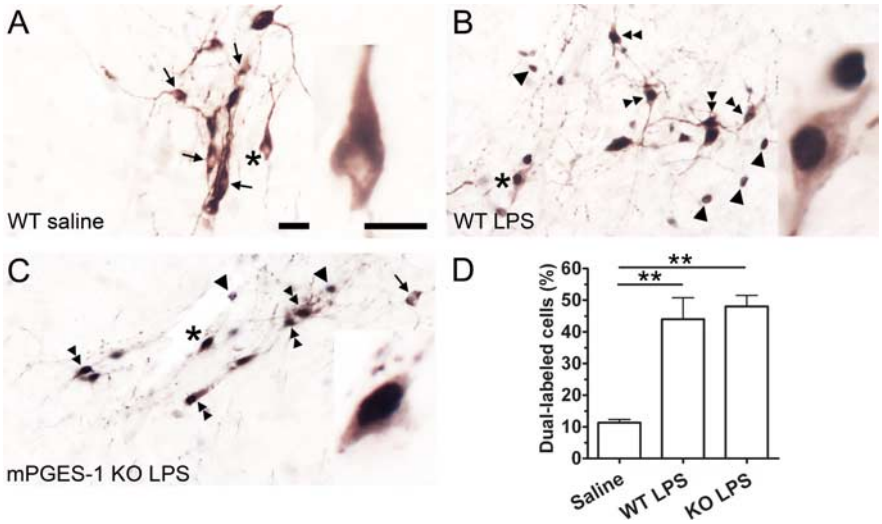

Figure 8. Similar immune-induced activation of catecholaminergic neurons in the ventrolateral medulla in wild-type (WT) and mPGES-1 KO mice, 3 h after intraperitoneal injection of 2 μg of LPS. ***A–C***, Dual-labeling immunohistochemistry in WT mice injected with saline (***A***), WT mice injected with LPS (***B***), and mPGES-1 KO mice injected with LPS (***C***). Catecholaminergic neurons (arrows) are stained for tyrosine hydroxylase immunoreactivity in the cytoplasm (brown reaction product), and activated neurons (arrowheads) are identified by Fos protein expression in the cell nucleus (black reaction product). The double arrowheads point at dual-labeled cells. The asterisks indicate neurons shown at higher magnification in insets. Scale bars, 50 and 25 μm (inset), respectively. ***D***, Percentage of tyrosine hydroxylase-positive neurons in the ventrolateral medulla that were colabeled for Fos. $n = 3–4$. Error bars indicate SEM. $^{**}p < 0.01$.

References

Althaus HH, Siepl C (1997) Oligodendrocytes isolated from adult pig brain synthesise and release prostaglandins. Cell Tissue Res 287:135–141.

Besedovsky H, del Rey A, Sorkin E, Dinarello CA (1986) Immunoregulatory feedback between interleukin-1 and glucocorticoid hormones. Science 233:652–654.

Buller K, Xu Y, Dayas C, Day T (2001) Dorsal and ventral medullary catecholamine cell groups contribute differentially to systemic interleukin-1beta-induced hypothalamic pituitary adrenal axis responses. Neuroendocrinology 73:129–138.

Cao C, Matsumura K, Yamagata K, Watanabe Y (1998) Cyclooxygenase-2 is induced in brain blood vessels during fever evoked by peripheral or central administration of tumor necrosis factor. Brain Res Mol Brain Res 56:45–56.

Ching S, Zhang H, Belevych N, He L, Lai W, Pu XA, Jaeger LB, Chen Q, Quan N (2007) Endothelial-specific knockdown of interleukin-1 (IL-1) type 1 receptor differentially alters CNS responses to IL-1 depending on its route of administration. J Neurosci 27:10476–10486.

Curran T, Morgan JI (1985) Superinduction of c-*fos* by nerve growth factor in the presence of peripherally active benzodiazepines. Science 229:1265–1268.

Dallaporta M, Pecchi E, Jacques C, Berenbaum F, Jean A, Thirion S, Troadec JD (2007) c-Fos immunoreactivity induced by intraperitoneal LPS administration is reduced in the brain of mice lacking the microsomal prostaglandin E synthase-1 (mPGES-1). Brain Behav Immun 21:1109–1121.

Dunn AJ, Chuluyan HE (1992) The role of cyclo-oxygenase and lipoxygenase in the interleukin-1-induced activation of the HPA axis: dependence on the route of injection. Life Sci 51:219–225.

Ek M, Kurosawa M, Lundeberg T, Ericsson A (1998) Activation of vagal afferents after intravenous injection of interleukin-1β: role of endogenous prostaglandins. J Neurosci 18:9471–9479.

Ek M, Arias C, Sawchenko P, Ericsson-Dahlstrand A (2000) Distribution of the EP3 prostaglandin E_2 receptor subtype in the rat brain: relationship to sites of interleukin-1-induced cellular responsiveness. J Comp Neurol 428:5–20.

Ek M, Engblom D, Saha S, Blomqvist A, Jakobsson PJ, Ericsson-Dahlstrand A (2001) Inflammatory response: pathway across the blood-brain barrier. Nature 410:430–431.

Elander L, Engström L, Hallbeck M, Blomqvist A (2007) IL-1beta and LPS induce anorexia by distinct mechanisms differentially dependent on microsomal prostaglandin E synthase-1. Am J Physiol Regul Integr Comp Physiol 292:R258–R267.

Elmquist JK, Ackermann MR, Register KB, Rimler RB, Ross LR, Jacobson CD (1993) Induction of Fos-like immunoreactivity in the rat brain following *Pasteurella multocida* endotoxin administration. Endocrinology 133:3054–3057.

Elmquist JK, Scammell TE, Jacobson CD, Saper CB (1996) Distribution of Fos-like immunoreactivity in the rat brain following intravenous lipopolysaccharide administration. J Comp Neurol 371:85–103.

Engblom D, Ek M, Ericsson-Dahlstrand A, Blomqvist A (2001) Activation of prostanoid EP_3 and EP_4 receptor mRNA-expressing neurons in the rat parabrachial nucleus by intravenous injection of bacterial wall lipopolysaccharide. J Comp Neurol 440:378–386.

Engblom D, Saha S, Engström L, Westman M, Audoly LP, Jakobsson PJ, Blomqvist A (2003) Microsomal prostaglandin E synthase-1 is the central switch during immune-induced pyresis. Nat Neurosci 6:1137–1138.

Engström L, Engblom D, Blomqvist A (2003) Systemic immune challenge induces preproenkephalin gene transcription in distinct autonomic structures of the rat brain. J Comp Neurol 462:450–461.

Engström L, Rosén K, Angel A, Fyrberg A, Mackerlova L, Konsman JP, Engblom D, Blomqvist A (2008) Systemic immune challenge activates an intrinsically regulated local inflammatory circuit in the adrenal gland. Endocrinology 149:1436–1450.

Ericsson A, Kovács KJ, Sawchenko PE (1994) A functional anatomical analysis of central pathways subserving the effects of interleukin-1 on stress-related neuroendocrine neurons. J Neurosci 14:897–913.

Ericsson A, Arias C, Sawchenko PE (1997) Evidence for an intramedullary prostaglandin-dependent mechanism in the activation of stress-related neuroendocrine circuitry by intravenous interleukin-1. J Neurosci 17:7166–7179.

Herman JP, Prewitt CM, Cullinan WE (1996) Neuronal circuit regulation of the hypothalamo-pituitary-adrenocortical stress axis. Crit Rev Neurobiol 10:371–394.

Hunt SP, Pini A, Evan G (1987) Induction of c-*fos*-like protein in spinal cord neurons following sensory stimulation. Nature 328:632–634.

Irie A, Sugimoto Y, Namba T, Harazono A, Honda A, Watabe A, Negishi M, Narumiya S, Ichikawa A (1993) Third isoform of the prostaglandin-E-receptor EP3 subtype with different C-terminal tail coupling to both stimulation and inhibition of adenylate cyclase. Eur J Biochem 217:313–318.

Katsuura G, Gottschall PE, Dahl RR, Arimura A (1988) Adrenocorticotropin release induced by intracerebroventricular injection of recombinant human interleukin-1 in rats: possible involvement of prostaglandin. Endocrinology 122:1773–1779.

Katsuura G, Arimura A, Koves K, Gottschall PE (1990) Involvement of organum vasculosum of lamina terminalis and preoptic area in interleukin 1 beta-induced ACTH release. Am J Physiol 258:E163–E171.

Knudsen PJ, Dinarello CA, Strom TB (1986) Prostaglandins posttranscriptionally inhibit monocyte expression of interleukin 1 activity by increasing intracellular cyclic adenosine monophosphate. J Immunol 137:3189–3194.

Krymskaya LG, Gromykhina NYu, Kozlov VA (1987) Interleukin 1 effect on adrenal gland function in mice. Immunol Lett 15:307–309.

Kunkel SL, Spengler M, May MA, Spengler R, Larrick J, Remick D (1988)

Prostaglandin E2 regulates macrophage-derived tumor necrosis factor gene expression. J Biol Chem 263:5380–5384.

Lacroix S, Rivest S (1997) Functional circuitry in the brain of immune-challenged rats: partial involvement of prostaglandins. J Comp Neurol 387:307–324.

Lacroix S, Valliéres L, Rivest S (1996) c-*fos* mRNA pattern and corticotropin-releasing factor neuronal activity throughout the brain of rats injected centrally with a prostaglandin of E2 type. J Neuroimmunol 70:163–179.

Langenbach R, Morham SG, Tiano HF, Loftin CD, Ghanayem BI, Chulada PC, Mahler JF, Davis BJ, Lee CA (1997) Disruption of the mouse cyclooxygenase 1 gene. Characteristics of the mutant and areas of future study. Adv Exp Med Biol 407:87–92.

Lazarus M, Yoshida K, Coppari R, Bass CE, Mochizuki T, Lowell BB, Saper CB (2007) EP3 prostaglandin receptors in the median preoptic nucleus are critical for fever responses. Nat Neurosci 10:1131–1133.

Luckman SM, Dyball RE, Leng G (1994) Induction of c-*fos* expression in hypothalamic magnocellular neurons requires synaptic activation and not simply increased spike activity. J Neurosci 14:4825–4830.

Marvel FA, Chen CC, Badr N, Gaykema RP, Goehler LE (2004) Reversible inactivation of the dorsal vagal complex blocks lipopolysaccharide-induced social withdrawal and c-Fos expression in central autonomic nuclei. Brain Behav Immun 18:123–134.

Matsuoka Y, Furuyashiki T, Bito H, Ushikubi F, Tanaka Y, Kobayashi T, Muro S, Satoh N, Kayahara T, Higashi M, Mizoguchi A, Shichi H, Fukuda Y, Nakao K, Narumiya S (2003) Impaired adrenocorticotropic hormone response to bacterial endotoxin in mice deficient in prostaglandin E receptor EP1 and EP3 subtypes. Proc Natl Acad Sci U S A 100:4132–4137.

McCoy JG, Matta SG, Sharp BM (1994) Prostaglandins mediate the ACTH response to interleukin-1-beta instilled into the hypothalamic median eminence. Neuroendocrinology 60:426–435.

Morham SG, Langenbach R, Loftin CD, Tiano HF, Vouloumanos N, Jennette JC, Mahler JF, Kluckman KD, Ledford A, Lee CA, Smithies O (1995) Prostaglandin synthase 2 gene disruption causes severe renal pathology in the mouse. Cell 83:473–482.

Morimoto A, Watanabe T, Morimoto K, Nakamori T, Murakami N (1991) Possible involvement of prostaglandins in psychological stress-induced responses in rats. J Physiol 443:421–429.

Nasushita R, Watanobe H, Takebe K (1997) A comparative study of adrenocorticotropin-releasing activity of prostaglandins E1, E2, F2 alpha and D2 in the rat. Prostaglandins Leukot Essent Fatty Acids 56:165–168.

Nilsberth C, Elander L, Hamzic N, Norell M, Lonn J, Engström L, Blomqvist A (2008) The role of IL-6 in LPS-induced fever by mechanisms independent of prostaglandin-E2. Endocrinology. Advance online publication. Retrieved January 14, 2009. doi:10.1210/en.2008–0806.

Oka T, Oka K, Scammell TE, Lee C, Kelly JF, Nantel F, Elmquist JK, Saper CB (2000) Relationship of EP(1–4) prostaglandin receptors with rat hypothalamic cell groups involved in lipopolysaccharide fever responses. J Comp Neurol 428:20–32.

Pecchi E, Dallaporta M, Thirion S, Salvat C, Berenbaum F, Jean A, Troadec JD (2006) Involvement of central microsomal prostaglandin E synthase-1 in IL-1beta-induced anorexia. Physiol Genomics 25:485–492.

Reyes TM, Walker JR, DeCino C, Hogenesch JB, Sawchenko PE (2003) Categorically distinct acute stressors elicit dissimilar transcriptional profiles in the paraventricular nucleus of the hypothalamus. J Neurosci 23:5607–5616.

Rivest S, Laflamme N, Nappi RE (1995) Immune challenge and immobilization stress induce transcription of the gene encoding the CRF receptor in selective nuclei of the rat hypothalamus. J Neurosci 15:2680–2695.

Ruud J, Blomqvist A (2007) Identification of rat brainstem neuronal structures activated during cancer-induced anorexia. J Comp Neurol 504:275–286.

Sagar SM, Price KJ, Kasting NW, Sharp FR (1995) Anatomic patterns of Fos immunostaining in rat brain following systemic endotoxin administration. Brain Res Bull 36:381–392.

Saha S, Engström L, Mackerlova L, Jakobsson PJ, Blomqvist A (2005) Impaired febrile responses to immune challenge in mice deficient in microsomal prostaglandin E synthase-1. Am J Physiol Regul Integr Comp Physiol 288:R1100–R1107.

Sawchenko PE, Swanson LW (1982) The organization of noradrenergic pathways from the brainstem to the paraventricular and supraoptic nuclei in the rat. Brain Res 257:275–325.

Schiltz JC, Sawchenko PE (2007) Specificity and generality of the involvement of catecholaminergic afferents in hypothalamic responses to immune insults. J Comp Neurol 502:455–467.

Trebino CE, Stock JL, Gibbons CP, Naiman BM, Wachtmann TS, Umland JP, Pandher K, Lapointe JM, Saha S, Roach ML, Carter D, Thomas NA, Durtschi BA, McNeish JD, Hambor JE, Jakobsson PJ, Carty TJ, Perez JR, Audoly LP (2003) Impaired inflammatory and pain responses in mice lacking an inducible prostaglandin E synthase. Proc Natl Acad Sci U S A 100:9044–9049.

Turnbull AV, Rivier CL (1999) Regulation of the hypothalamic-pituitary-adrenal axis by cytokines: actions and mechanisms of action. Physiol Rev 79:1–71.

Vasilache AM, Andersson J, Nilsberth C (2007) Expression of PGE_2 EP_3 receptor subtypes in the mouse preoptic region. Neurosci Lett 423:179–183.

Wan W, Janz L, Vriend CY, Sorensen CM, Greenberg AH, Nance DM (1993) Differential induction of c-Fos immunoreactivity in hypothalamus and brain stem nuclei following central and peripheral administration of endotoxin. Brain Res Bull 32:581–587.

Wan W, Wetmore L, Sorensen CM, Greenberg AH, Nance DM (1994) Neural and biochemical mediators of endotoxin and stress-induced c-*fos* expression in the rat brain. Brain Res Bull 34:7–14.

Watanabe T, Morimoto A, Sakata Y, Murakami N (1990) ACTH response induced by interleukin-1 is mediated by CRF secretion stimulated by hypothalamic PGE. Experientia 46:481–484.

Watanobe H, Nasushita R, Sasaki S, Suda T (1998) Evidence that a fast, rate-sensitive negative feedback effect of corticosterone is not a principal mechanism underlying the indomethacin inhibition of interleukin-1 beta-induced adrenocorticotropin secretion in the rat. Cytokine 10:377–381.

Watts AG (2005) Glucocorticoid regulation of peptide genes in neuroendocrine CRH neurons: a complexity beyond negative feedback. Front Neuroendocrinol 26:109–130.

Weidenfeld J, Siegel RA, Conforti N, Chowers I (1983) ACTH and corticosterone secretion following indomethacin, in intact, adrenalectomized and dexamethasone-pretreated male rats. Neuroendocrinology 36:49–52.

Weidenfeld J, Abramsky O, Ovadia H (1989) Evidence for the involvement of the central adrenergic system in interleukin 1-induced adrenocortical response. Neuropharmacology 28:1411–1414.

Zhang J, Rivest S (1999) Distribution, regulation and colocalization of the genes encoding the EP2- and EP4-PGE2 receptors in the rat brain and neuronal responses to systemic inflammation. Eur J Neurosci 11:2651–2668.

Zhang YH, Lu J, Elmquist JK, Saper CB (2003) Specific roles of cyclooxygenase-1 and cyclooxygenase-2 in lipopolysaccharide-induced fever and Fos expression in rat brain. J Comp Neurol 463:3–12.